ELSEVIER

Fusion Engineering and Design 26 (1995) 185–190

Fusion Engineering and Design

A study of three-half-turn and frame antennae for ion cyclotron range of frequency plasma heating in the URAGAN-3M torsatron

A.I. Lysoivan, V.E. Moiseenko, V.V. Plyusnin, S.V. Kasilov, V.N. Bondarenko, V.V. Chechkin, I.P. Fomin, L.I. Grigor'eva, V.G. Konovalov, S.V. Koval'ov, A.P. Litvinov, Yu.K. Mironov, N.I. Nazarov, O.S. Pavlichenko, R.O. Pavlichenko, A.N. Shapoval, A.I. Skibenko, E.D. Volkov

Institute of Plasma Physics, National Science Center, Kharkov Institute of Physics and Technology, 310108 Kharkov, Ukraine

Abstract

Numerical and experimental results of Alfvén wave heating of plasmas in the frequency range below the ion cyclotron frequency ($\omega < \omega_{ci}$) are presented. Two different types of antenna were used for plasma production and heating: a frame type antenna (FTA) conventionally used in the URAGAN-3M device and a three-half-turn antenna (THTA) proposed recently to avoid the deleterious effects of conversion of fast wave to slow wave in the plasma periphery and to perform plasma core heating more effectively. Numerical modeling of electromagnetic field excitation in the URAGAN-3M plasma by the FTA and THTA was performed using a one-dimensional code. The results of calculations showed better performance of the compact THTA compared with the FTA for the case of a high density plasma (approximately 10^{13} cm^{-3}). When using the THTA, the experiments performed showed the possibility of dense plasma production (more than 2×10^{13} cm^{-3}) and heating, which had not been obtained earlier in the URAGAN-3M. Shifting the power deposition profile deeper inside the plasma body with the THTA resulted in modification of the plasma density profile and an improvement in plasma confinement.

1. Introduction

The basis of Alfvén wave heating of plasmas in the frequency range below the ion cyclotron frequency ($\omega < \omega_{ci}$) is the mechanism of fast wave (FW) conversion into a strongly damped slow wave (SW) in the region of the Alfvén resonance (AR) layer. The AR condition, $k_{\parallel}^2 \approx n^2/R^2 \approx (\omega^2/c^2)\bar{\varepsilon}_{11}$ (where n is the longitudinal mode number, R is the major radius of the torus, $\bar{\varepsilon}_{11}$ is the dielectric tensor component averaged over the magnetic surface), may be fulfilled at different magnetic surfaces. Alfvén wave heating is most efficient when the modes are used for which $k_{\parallel}a \approx \pi$. This condition follows from the calculations presented in Refs. [1,2] and is formulated explicitly in Ref. [3]. The necessity of excitation of modes with large toroidal numbers $n_{opt} \approx \pi R/a$

Elsevier Science S.A.
SSDI 0920-3796(94)00185-5

follows from this condition. Note that the influence of the poloidal component of the confining magnetic field on these modes is negligible. In addition to Alfvén resonance for the modes with $|n| = n_{opt}$, a large amount of resonance for modes with $|n| = 1$ to $|n| = n_{max} \geqslant n_{opt}$ can be excited. It should be mentioned that the lower the value of n, the nearer to the plasma edge the AR layer is located. Therefore the modes with low n numbers can be considered parasitic and their excitation must be suppressed. This problem was solved by using helical [4–6] and multi-half-turn [7] antennae which excite only one Alfvén resonance. However, these antennae have a very complicated and bulky design, that prevents their wide use in experiments. Another disadvantage is the sensitivity of the power deposition profile and plasma loading resistance to the variations in plasma density resulting from the AR condition. These shortcomings caused the search for Alfvén heating scenarios with compact antennae [8].

In Ref. [3] a compact three-half-turn antenna (THTA) was proposed for AR heating of toroidal plasmas. Because of its small size, this antenna excites all toroidal modes. However, excitation of the edge resonances with low n numbers is considerably suppressed (in a more effective manner than by a two-strap antenna [8]), while a large amount of modes with $|n| \approx n_{opt}$ are efficiently excited. The insensitvity of this antenna to the variations in plasma density does not result from single AR surface shifting, but from multiple resonances excited in a relay race regime [9]. Therefore the power deposition profile and loading resistance of the THTA are weakly dependent on the plasma density.

In accordance with the results of Ref. [3], a variant of the THTA adapted to the URAGAN-3M torsatron was designed, manufactured and installed in the device together with the conventional frame-type antenna (FTA) [10] (neither antenna has a Faraday shield and both are coated with a thin layer of TiN). It should be mentioned that the frequency for Alfvén wave heating by these antennae is close to the ion cyclotron frequency because the URAGAN-3M torsatron is a small device.

In this paper, the results of numerical modeling of r.f. plasma heating in the URAGAN-3M torsatron with the FTA and THTA along with the first THTA experiments are presented.

2. Numerical model

Numerical modeling of the r.f. fields in plasma excited by external antennae was performed using a one-dimensional wave code. The toroidal geometry is simulated by the cylindrical approximation via the periodicity in the cylindrical axis direction. The model used takes into account the excitation of SW as well as FW, collisional and collisionless absorption of the waves by electrons and ions, and a finite value of ω/ω_{ci}. The stationary magnetic field B_0 was assumed to be inhomogeneous in the radial direction. The antennae are modeled by the external currents flowing along narrow strip conductors.

Antennae FTA and THTA are shown in Fig. 1. The specific feature of the THTA design used in the URAGAN-3M is that the three half-turns are connected to each other by longitudinal conductors positioned near the conducting walls (not shown). The sizes of the antennae are as follows: $l_z = 70$ cm and $l_\varphi = 23$ cm for the FTA, $l_z = 24$ cm and $l_\varphi = 40$ cm for the THTA (here l_z and l_φ are the antenna dimensions in the toroidal and poloidal directions respectively).

The calculations were performed for the parameters given below, which correspond to one of the URAGAN-3M operational regimes: major radius $R = 100$ cm, wall radius $r_w = 19$ cm, average plasma radius $\bar{a} = 12$ cm, toroidal magnetic field $B_0(0) = 0.47$ T, central electron and ion temperatures $T_e(0) = T_i(0) = 50$ eV, $\omega/\omega_{ci} = 0.78$. The FTA and THTA were positioned at radii $r_{a1} = 16$ cm and $r_{a2} = 14.5$ cm respectively. The plasma density and temperature profiles are assumed to be close to the profiles observed experimentally. The presence of the peripheral plasma in the antenna vicinities is also taken into account.

3. Numerical and experimental results

The computed r.f. power deposition profiles onto the electrons P_e for two values of plasma

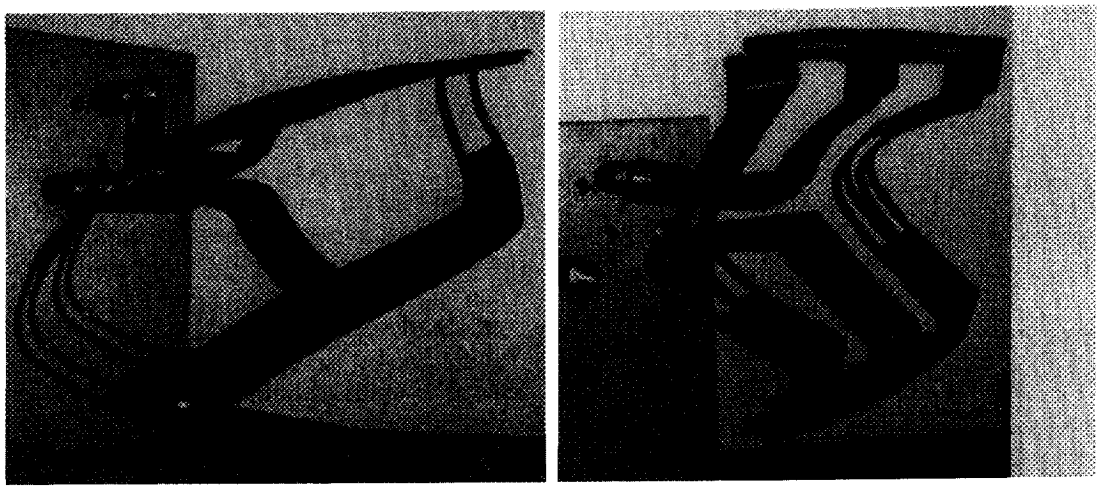

Fig. 1. View of the frame type (a) and three-half-turn (b) antennae installed in the URAGAN-3M device.

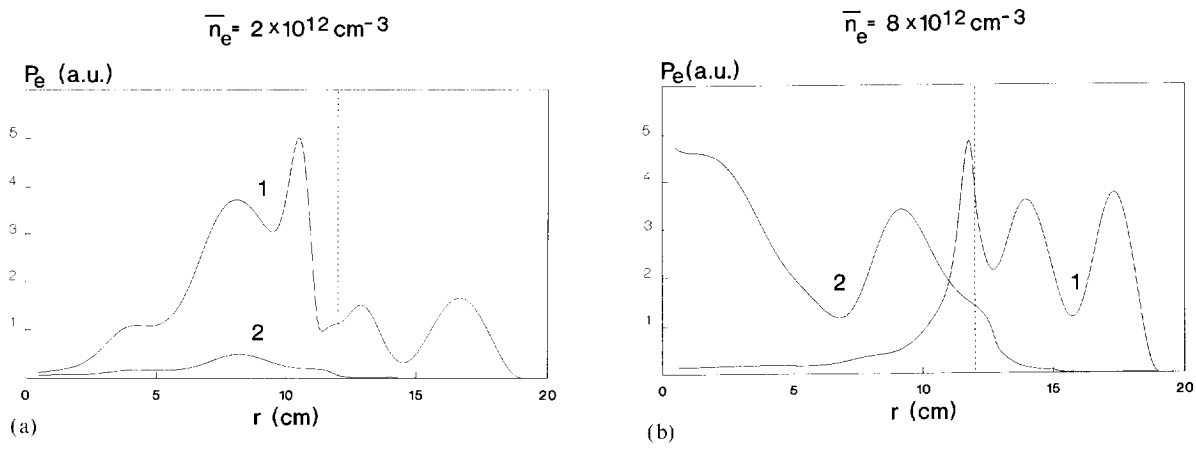

Fig. 2. The power deposition profile onto the electrons produced by the one-dimensional wave code for FTA (curve 1) and THTA (curve 2) in two cases: (a) low density ($n_e = 2 \times 10^{12}\,cm^{-3}$); (b) high density ($n_e = 8 \times 10^{12}\,cm^{-3}$). The dashed line indicates the plasma radius.

density are plotted in Fig. 2. (The r.f. power deposited onto the ions is substantially less than that deposited onto the electrons for these regimes.) In the low density case ($n_e = 2 \times 10^{12}\,cm^{-3}$), the maxima of the r.f. power density absorbed are positioned inside the plasma body for both antennae. It should be noted that the r.f. power coupled by the FTA is several times greater than that coupled by the THTA.

In the higher density case ($n_e = 8 \times 10^{12}\,cm^{-3}$), the power deposition profile for the THTA improves; the total value of absorbed power also increases owing to the rise in plasma loading resistance. The FTA deposits r.f. power mainly outside the plasma column owing to the excitation of long-wavelength modes. These modes do not penetrate into the plasma core and form global resonances in the peripheral plasma. The non-monotonic behavior of the FTA parameters (average radius of r.f. power deposition, plasma loading resistance, etc.) vs. plasma density is caused by this effect. For the THTA, the excita-

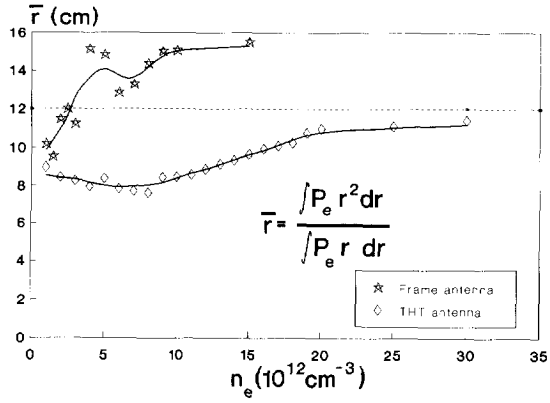

Fig. 3. The computed averaged radius of deposited r.f. power vs. plasma density for both antennae. The plasma radius is marked by the dashed line.

tion of long-wavelength modes is suppressed essentially for all density values.

The computed average radius of the r.f. power deposition vs. plasma density for both antennae is shown in Fig. 3. The power deposition for the FTA is localized in the plasma bulk only for low values of plasma density ($n_e \approx 2 \times 10^{12}\ \mathrm{cm}^{-3}$) and shifts outside the plasma body with increasing plasma density. In the case of the THTA, the power deposition profile is always more central. The average radius of power deposition depends weakly on the plasma density and, without exceeding the plasma radius, reaches a smooth minimum at the density $n_e \approx 7 \times 10^{12}\ \mathrm{cm}^{-3}$.

R.f. breakdown and plasma production were performed usually by the FTA. Plasma production by the THTA alone was not observed. Therefore the r.f. pulse of the FTA (RF-1) preceded that of the THTA (RF-2) in the experiments. In order to find the plasma density threshold for THTA operation, a special series of experiments was performed. In this series, the time delay between the end of RF-1 and start of RF-2 pulses was varied. In so doing, the initial $\bar{n}_e$ value (line-averaged plasma density measured through the central chord) for the THTA also varied. It was observed that when $\bar{n}_e < 4 \times 10^{11}\ \mathrm{cm}^{-3}$ (defined as the threshold value) the THTA r.f. pulse does not support the discharge. This means that the THTA weakly heats the low density plasma, as predicted by theoretical study.

In typical discharges, the growth of plasma density during the RF-1 pulse saturated at a level of order $\bar{n}_e < (4-7) \times 10^{12}\ \mathrm{cm}^{-3}$. During THTA operation the substantial increase in $\bar{n}_e$ up to $3 \times 10^{13}\ \mathrm{cm}^{-3}$ was observed at approximately the same r.f. power [11]. It should be mentioned that the experiments on the URAGAN-3M device are performed for two regimes of neutral gas filling. In the first regime, the gas pressure is kept constant in the vacuum tank surrounding the plasma and vacuum magnetic field coils. In the second regime, pulsed gas puffing during the plasma discharge is used. In both cases the neutral gas flux into the plasma column is considerable. The stationary level of plasma density can be understood in terms of a balance between the ionization rate and diffusion losses. The different values of stationary density for the RF-1 and RF-2 pulses may be explained by the different energy deposition profiles of the antennae.

Fig. 4 presents the temporal evolutions of some plasma parameters illustrating dense plasma ($\bar{n}_e < 2 \times 10^{13}\ \mathrm{cm}^{-3}$) heating when the r.f. power (approximately 100 kW) was input by the THTA. The use of neutral gas (H_2) puffing and long-term r.f. conditioning resulted in an improvement in the discharge. The impurity content decreased and plasmas of higher parameters were obtained compared with the early phase of r.f. experiments [11].

The transition to a qualitatively new state of plasma discharge was observed during the THTA pulse (RF-2) as opposed to the FTA pulse (RF-1) (Fig. 4). The line-averaged plasma density increased during the RF-2 pulse mainly in the plasma core (chord 3) but not in the periphery (chord 1) (Fig. 4(a)), while the signal of the H_β line measured outside the plasma core decreased a little (Fig. 4(b)). The ion saturation current registered by external Langmuir probes dropped sharply (Fig. 4(d)) and the plasma density profile steepened near the edge (Fig. 5). No direct measurements of electron temperature were taken in these experiments. However, the electron temperature can be estimated as $T_e \approx 50$ eV from the $C\bar{V}$-line signal (Fig. 4(c)). It should be noted that this signal peaked in the plasma core. Such behavior of plasma parameters has never been registered using the FTA at any r.f. power level and

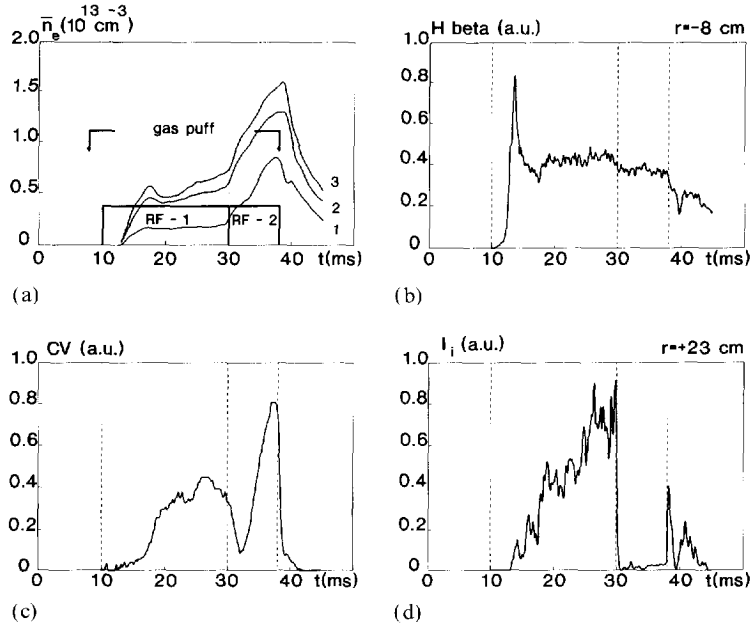

Fig. 4. Time traces of (a) $\langle n_e \rangle$, (b) the H_β-line, (c) the $C\bar{V}$-line, and (d) I_i (ion saturation current on an external Langmuir probe), with successive operation of FTA (RF-1) and THTA (RF-2) for shot 57 138 ($B_0(0) = 0.47$ T, $P_{RF\text{-}1} \approx P_{RF\text{-}2} \approx 100$ kW, $f_1 \approx f_2 \approx 5.6$ MHz).

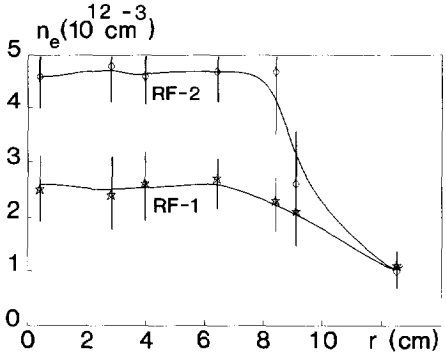

Fig. 5. Experimental plasma density profiles for FTA (curve 1, $P_{RF\text{-}1} \approx 200$ kW) and THTA (curve 2, $P_{RF\text{-}2} \approx 100$ kW) operation respectively.

may be caused by more central energy deposition in the case of the THTA and consequent modification of the plasma density and the temperature profile.

The observed phenomena are very similar to H-mode-like regimes discovered earlier in the stellarators W 7-AS [12] and compact helical system (CHS) [13] with auxiliary heating of dense plasma ($\bar{n}_e \approx (4-5) \times 10^{13}$ cm^{-3}). The rise in density in Fig. 4(a) is undoubtedly related to that observed previously in the TCA [14].

4. Summary

The scheme of Alfvén wave heating of plasma using a THTA proposed previously for large-scale fusion machines has been realized in the URAGAN-3M torsatron. The first experiments with this antenna have shown the possibility of dense plasma production ($\bar{n}_e > 2 \times 10^{13}$ cm^{-3}) not obtained earlier in this device. At a moderate r.f. power level (about 100 kW), the new antenna provides dense plasma build-up and heating. Transition to the regime with improved plasma confinement was observed and is now under investigation.

Numerical modeling of electromagnetic field excitation in the URAGAN-3M torsatron by the FTA and THTA was performed using a one-di-

mensional wave code. The results of the calculations were found to be in satisfactory agreement with the experimental data. They have made clearer the physics of Alvén wave heating with both antennae at low and high plasma densities. From experiments and numerical modeling, the scheme of Alfvén wave heating with a THTA seems very promising.

Acknowledgement

This work was supported by the Ukrainian State Committee on Science and Technology under Contract No 9.02.02/094-93.

References

[1] S. Puri, Antenna optimization for Alfvén wave heating, Nucl. Fusion, 27 (1987) 229–239.

[2] S. Puri, Role of plasma equilibrium current in Alfvén wave antenna optimization, Nucl. Fusion, 27 (1987) 1091–1104.

[3] V.E. Moiseenko, Alfvén heating in toroidal plasmas by using three-half-turn antenna. 8th Stellarator Workshop, IAEA, Vienna, 1991, pp. 207–210.

[4] R.A. Demirkhanov, A.G. Kirov, S.N. Lozovskij et al., Plasma heating in a toroidal system by a helical quadrupole RF field with $\omega < \omega_{ci}$. 6th Int. Conf. on Plasma Physics and Controlled Nuclear Fusion Research, Vol. III, IAEA, Vienna, 1977, pp. 31–37.

[5] S.N. Golovato and J.L. Shohet, Plasma heating by Alfvén wave excitation in the Proto-Cleo stellarator, Phys. Fluids, 21 (1978) 1421–1427.

[6] K. Uo, A. Iiyoshi, H. Akimune et al., RF heating experiments on Heliotron devices and analysis of equilibrium and stability of straight helical Heliotron plasma. 7th Int. Conf. on Plasma Physics and Controlled Nuclear Fusion Research, Vol. II, IAEA, Vienna, 1979, pp. 323–334.

[7] A. de Chambrier, A.D. Cheetham, A. Heym et al., Alfvén wave coupling experiments on the TCA tokamak, Plasma Phys., 24 (1982) 893–902.

[8] R. Majeski, P. Probert, P. Moroz et al., Alfvén wave experiments in the Phaedrus-T tokamak, Phys. Fluids B, 5 (1993) 2506–2512.

[9] A.I. Lysoivan, V.E. Moiseenko, O.M. Shvets and K.N. Stepanov, Analysis of ICRF ($\omega \leqslant \omega_{ci}$) plasma production in large scale tokamaks, Nucl. Fusion, 32 (1992) 1361–1372.

[10] O.M. Shvets, I.A. Dikij, S.S. Kalinichenko et al., Absorption of Alfvén waves and plasma production in the OMEGA and URAGAN-3 toroidal devices, Nucl. Fusion, 26 (1986) 23–41.

[11] S.V. Kasilov, A.I. Lysoivan, E. Moiseenko and V.V. Plyusnin, Performance of three-half-turn and frame antennas for ICRF plasma heating in URAGAN-3M torsatron. 9th Stellarator Workshop, IAEA, Vienna, 1993, pp. 447–452.

[12] V. Erckmann, R. Brakel, R. Burhenn et al., H-mode like transition in the W 7-AS stellarator with high power 140 GHz ECRH. 14th Int. Conf. on Plasma Physics and Controlled Nuclear Fusion Research, Vol. II, IAEA, Vienna, 1993, pp. 469–481.

[13] K. Toi, S. Okamura, H. Iguchi et al., Formation of an H-mode-like transport barrier in the CHS heliotron/torsatron. 14th Int. Conf. on Plasma Physics and Controlled Nuclear Fusion Research, Vol. II, IAEA, Vienna, 1993, pp. 461–468.

[14] G.G. Borg and B. Joye, Parasitic antenna loading measurements and comparison between shielded and unshielded antenna excitation during Alfvén wave heating in TCA, Nucl. Fusion, 32 (1992) 801–813.